

On Topological Entropy of Finite Representations of the Hénon map

Zbigniew Galias

*Department of Electrical Engineering,
AGH University of Science and Technology,
Mickiewicza 30, 30-059 Kraków, Poland
galias@agh.edu.pl*

The topological entropy of finite representations of the Hénon map is studied. Efficient methods to compute the topological entropy of finite representations of maps are presented. Accurate finite representations of the Hénon map and its iterates are constructed and the topological entropy of these representations is calculated. The relation between the topological entropy of the Hénon map and the topological entropy of its finite representations is discussed.

Keywords: topological entropy, Hénon map.

1. Introduction

The topological entropy of a continuous map is a non-negative number characterizing the complexity of trajectories of this map [Adler *et al.*, 1965; Dinaburg, 1971; Bowen, 1971]. It measures the exponential growth rate in time of the number of trajectories which can be distinguished from each other at a certain observation precision in the limit when the precision goes to zero. Topological entropy is one of the most important characterizations of dynamical systems. It is used to define the notion of the topological chaos. A dynamical system is called chaotic in the topological sense if its topological entropy is positive. Topological entropy is used to characterize nonlinear systems in many applications such as random number generators [Zhou *et al.*, 2006; Cicek *et al.*, 2017], secure communication systems [Guo *et al.*, 2018] or chaos based encryption methods [Akgul *et al.*, 2013; Qi *et al.*, 2016].

Computation of topological entropy directly from the definition is usually difficult due to limits involved. In this work, we present efficient methods to compute the topological entropy of finite representations of maps. Finite representations, also called “graph representations of the dynamics” belong to standard interval arithmetic based rigorous numerical tools to analyze nonlinear dynamical systems [Dellnitz *et al.*, 1997; Zgliczyński, 1997; Galias, 2001; Day *et al.*, 2008]. Interval arithmetic is used to control the influence of rounding errors, which are inevitable in computer-assisted studies of dynamical systems. The standard method to represent the dynamics of a system over a trapping region or over an attractor is to cover the set under study by interval vectors (boxes) and to find possible transitions between boxes. Possible transitions are usually represented in the form of a transition matrix. The set of boxes covering an attractor and the corresponding transition matrix define a finite representation. It is therefore an interesting problem what is the relation between the topological entropy of the dynamical system and the topological entropy of its finite precision representation. This problem is also important from a practical point of view since in applications finite precision representations of nonlinear maps are used instead of infinite precision formulations.

In this work, we propose efficient methods to compute the topological entropy of finite representations

of maps. As an example, we consider the Hénon map $h(x, y) = (1 + y - ax^2, bx)$ with the classical parameter values $a = 1.4$, $b = 0.3$ [Hénon, 1976]. Accurate finite representations of the Hénon map and its iterates are constructed and their topological entropy is calculated.

The problems how to calculate the topological entropy $H(h)$ of the Hénon map with the classical parameter values, how to find rigorous lower and upper bounds on $H(h)$ and how the topological entropy changes with parameter values have been studied extensively over the last 40 years. A method to calculate the topological entropy based on estimating the logarithmic growth of certain curves is presented and an estimate $H(h) \approx 0.4640$ is obtained in [Newhouse & Pignataro, 1993]. Three numerical methods to estimate the topological entropy are presented in [Jacobs *et al.*, 1998]. The most accurate of these three methods is based on averaging stretching rates of trajectories and yields an estimate $H(h) \in [0.46490, 0.46496]$. The topological entropy of the Hénon map is studied by means of pruning fronts in [D'Alessandro *et al.*, 1999]. The construction starts with a binary partition obtained by considering primary tangencies between stable and unstable manifolds [Grassberger & Kantz, 1985]. Pruning fronts are found and based on the number of allowed sequences the topological entropy is estimated as $H(h) \approx 0.4651$. The relation between the topological entropy estimate and the choice of the partition using the Hénon map as one of the examples is studied in [Boltt *et al.*, 2001]. A rigorous method to compute upper bounds on the topological entropy of a map with respect to a partition of the state space is given in [Froyland *et al.*, 2001]. Applying this method to the partition constructed by joining primary homoclinic tangencies yields 0.4687 and provides an upper bound $H(h) < 0.4687$. Using symbolic sequences of length 10^6 it is estimated in [Hirata & Mees, 2003] that the topological entropy of the Hénon map belongs to $[0.46482, 0.46497]$. The existence of several regions of hyperbolic parameters in the parameter space of the Hénon map is proved in [Arai, 2007]. Lower bounds on the topological entropy for 43 hyperbolic plateaus of the Hénon map are computed in [Frongillo, 2014].

Let us now recall several results regarding the estimates of the topological entropy of the Hénon map based on the number of periodic orbits. Under certain assumptions the relation between the topological entropy of the map f and the number of periodic orbits is $H(f) = \lim_{n \rightarrow \infty} n^{-1} \log(P_n)$, where P_n is the number of fixed points of f^n . Therefore the expression $H_n = n^{-1} \log(P_n)$ is often used to estimate the topological entropy based on the number of periodic orbits. In [Auerbach *et al.*, 1987], using the Newton-Raphson method periodic orbits with the period $p \leq 12$ are found and the topological entropy is estimated as $H_{12} = 0.459$. A systematic method to detect all low-period orbits for the Hénon map is proposed in [Biham & Wenzel, 1989]. The method is applied to find all period- p orbits with $p \leq 28$, and an estimate $H_{28} = 0.46485$ is obtained. The Biham-Wenzel method is based on the construction of artificial dynamical systems with stable fixed points corresponding to periodic orbits of the Hénon map. This method is not theoretically justified and may produce wrong results as shown in [Grassberger *et al.*, 1989]. Surprisingly, it works correctly for the classical parameter values at least for short periodic orbits considered in [Biham & Wenzel, 1989]. Rigorous interval computations are carried out in [Galias, 2001] to find all periodic orbits with periods $p \leq 30$. It is confirmed that the results reported in [Biham & Wenzel, 1989] for $p \leq 28$ are correct and an estimate $H_{30} = 0.46495$ is obtained. Using the Biham-Wenzel method combined with a pruning technique period- p orbits with $p \leq 50$ are found in [Galias & Tucker, 2015]. The estimates H_n obtained for $36 \leq n \leq 50$ satisfy the conditions $H_n \in [0.4649324, 0.4649374]$, which indicates that in the estimate $H(h) \approx 0.46493$ all digits are correct.

In the literature, there are several results on rigorous lower bounds on the topological entropy of the Hénon map. The existence of a transversal homoclinic point for the Hénon map is proved in [Misiurewicz & Szewc, 1980]. It follows that the Hénon map supports the Smale's horseshoe dynamics for some unknown iterate of h [Robinson, 1995]. A computer assisted proof of the existence of the horseshoe dynamics for the h^{25} is given in [Stoffer & Palmer, 1999]. Using the method of covering relations it is shown in [Zgliczyński, 1997] that h^7 supports the full shift dynamic on two symbols. It follows that $H(h) > 0.099$. The method of covering relations is used in [Galias & Zgliczyński, 2001] to prove that $H(h) > 0.3381$ and in [Galias, 2002] to prove that $H(h) > 0.43$. In [Day *et al.*, 2008], algorithms to compute rigorous lower bound on the topological entropy based on Conley index theory are presented and a rigorous lower bound $H(h) > 0.432$ is found. The best lower bound known so far is presented in [Newhouse *et al.*, 2008], where enclosures of stable and unstable manifolds of unstable periodic points are used to show that $H(h) > 0.46469$.

It is more difficult to obtain a rigorous upper bound on $H(h)$. From the fact that the nonlinearity

in the definition of the Hénon map is quadratic it follows that $H(h) \leq \log(2) \approx 0.69315$ (see [Newhouse, 1988]). This bound is quite far from the expected value $H(h) \approx 0.46493$. A method to compute an upper bound on the difference between the topological entropy of a map and the topological entropy of its finite representation is proposed in [Yomdin, 1991]. It follows that knowing the topological entropy of the finite representation one may obtain nontrivial upper bounds on the topological entropy of the original map provided that the topological entropy of a finite representation is sufficiently close to the entropy of the map and that the representation is sufficiently accurate. In this context, this work is a step towards obtaining rigorous upper bounds on $H(h)$ by providing efficient methods to compute the topological entropy of finite representations.

2. Topological Entropy of Finite Representations of Maps

The first definition of the topological entropy of a map is introduced in [Adler *et al.*, 1965]. It is based on the idea to assign a number to measure size of an open cover and then take the supremum over all open covers. In this definition, we consider all open covers of the space X (in the following we will use $X = \mathbb{R}^m$). For two open covers \mathcal{C}_1 and \mathcal{C}_2 by $\mathcal{C}_1 \vee \mathcal{C}_2$ we denote the cover composed of all non-empty intersections of sets from \mathcal{C}_1 and \mathcal{C}_2 , i.e. $\mathcal{C}_1 \vee \mathcal{C}_2 = \{\mathcal{C}_1 \cap \mathcal{C}_2 : \mathcal{C}_1 \cap \mathcal{C}_2 \neq \emptyset, \mathcal{C}_1 \in \mathcal{C}_1, \mathcal{C}_2 \in \mathcal{C}_2\}$. $\mathcal{C}_1 \vee \mathcal{C}_2 \vee \dots \vee \mathcal{C}_n$ is defined recursively as $\mathcal{C}_1 \vee \mathcal{C}_2 \vee \dots \vee \mathcal{C}_n = \mathcal{C}_1 \vee (\mathcal{C}_2 \vee \dots \vee \mathcal{C}_n)$. For an open cover \mathcal{C} of X by $N(\mathcal{C})$ we denote the smallest number of elements of \mathcal{C} covering X . The *topological entropy* of a continuous map $f: X \mapsto X$ is defined as

$$H(f) = \sup_{\mathcal{C}} \lim_{n \rightarrow \infty} \frac{1}{n} \log N(\mathcal{C} \vee f^{-1}(\mathcal{C}) \vee \dots \vee f^{-n+1}(\mathcal{C})), \quad (1)$$

where the supremum is taken over all open covers \mathcal{C} of X . We use the natural logarithm although this choice is arbitrary and in some papers the binary logarithm is used.

The definition (1) is not convenient from the computational point of view. We will follow a definition using the notion of (n, ε) -separated sets, which is introduced in [Dinaburg, 1971] and independently in [Bowen, 1971].

We say that a subset E of X is (n, ε) -separated for the map f if for each $x, y \in E$ with $x \neq y$ there exist $i \in \{0, 1, 2, \dots, n-1\}$ such that $d(f^i(x), f^i(y)) \geq \varepsilon$, where $d(x, y)$ is the distance between x and y . The topological entropy of f is defined as

$$H(f) = \lim_{\varepsilon \rightarrow 0} \limsup_{n \rightarrow \infty} \frac{1}{n} \log s(f, n, \varepsilon), \quad (2)$$

where $s(f, n, \varepsilon)$ is the maximal cardinality of an (n, ε) -separated set for the map f .

An alternative definition is based on the notion of (n, ε) -spanning sets. We say that $E \subset X$ is an (n, ε) -spanning set for f if for every $x \in X$ there is $y \in E$ such that $d(f^i(x), f^i(y)) < \varepsilon$ for all $i \in \{0, 1, \dots, n-1\}$. The topological entropy of f is equal to

$$H(f) = \lim_{\varepsilon \rightarrow 0} \limsup_{n \rightarrow \infty} \frac{1}{n} \log r(f, n, \varepsilon), \quad (3)$$

where $r(f, n, \varepsilon)$ is the minimal cardinality of an (n, ε) -spanning set for the map f .

From the above definitions it follows that the topological entropy of f can be estimated by

$$H(f, n, \varepsilon) = \frac{1}{n} \log s(f, n, \varepsilon), \quad (4)$$

where n is sufficiently large, and ε is sufficiently small. In [Yomdin, 1991], an upper bound on the difference between $H(f, n, \varepsilon)$ and $H(f)$ is derived. Using this bound, one can obtain rigorous upper bounds on $H(f)$.

The finite precision approximation of the topological entropy of f with the precision ε is defined as

$$H(f, \varepsilon) = \lim_{n \rightarrow \infty} H(f, n, \varepsilon). \quad (5)$$

In this work, we present methods how to compute upper bounds on $H(f, n, \varepsilon)$ and $H(f, \varepsilon)$. Using the Hénon map h as an example, we study the relation between finite precision approximations $H(h, \varepsilon)$ and $H(h)$. We also study the problem of finding finite precision approximations $H(h^k, \varepsilon)$ for iterates of h , and show that this may lead to better upper bounds on the topological entropy of h .

2.1. Finite Representations

A set $\mathbf{v} = [k_1\varepsilon, (k_1 + 1)\varepsilon] \times [k_2\varepsilon, (k_2 + 1)\varepsilon] \times \cdots \times [k_m\varepsilon, (k_m + 1)\varepsilon] \subset \mathbb{R}^m$, where $\varepsilon > 0$ and k_1, k_2, \dots, k_m are integers is called an ε -box with the size ε . Let V be a cover of Ω by ε -boxes, i.e. $V = \{\mathbf{v}_j\}_{j=1}^N$ and $\Omega \subset \bigcup_{j=1}^N \mathbf{v}_j$, where N is the number of ε -boxes in the cover V . For the cover V , we define the transition matrix $A \in \mathbb{R}^{N \times N}$:

$$A_{j,i} = \begin{cases} 0 & \text{if } f(\mathbf{v}_j) \cap \mathbf{v}_i = \emptyset, \\ 1 & \text{if } f(\mathbf{v}_j) \cap \mathbf{v}_i \neq \emptyset. \end{cases} \quad (6)$$

The matrix A defines possible transition between ε -boxes. The pair (V, A) is called a *finite representation* of f over the set Ω with the accuracy ε . In practical applications, the number N of ε -boxes may be large (several millions). However, the transition matrix is usually sparse. To store the matrix A it is sufficient to remember for each $1 \leq j \leq N$ the set $D_j = \{i : A_{j,i} = 1\}$.

Let us first describe how to compute a finite representation of f over an attractor \mathcal{A} . We assume that $\Omega \subset \mathbb{R}^m$ contains the attractor \mathcal{A} . We start by covering Ω by ε -boxes \mathbf{v}_j . For each box \mathbf{v}_j we compute an enclosure \mathbf{w}_j of $f(\mathbf{v}_j)$ and find boxes \mathbf{v}_i which have non-empty intersection with \mathbf{w}_j . The evaluation of $f(\mathbf{v}_j)$ can be carried in interval arithmetic in which case the enclosure condition $f(\mathbf{v}_j) \subset \mathbf{w}_j$ is automatically satisfied. Note that if $A_{j,i} = 1$ then the transition in one iteration from \mathbf{v}_j to \mathbf{v}_i is not forbidden. In general $f(\mathbf{v}_j) \neq \mathbf{w}_j$ and in consequence it may happen that $A_{j,i} = 1$ and $f(\mathbf{v}_j) \cap \mathbf{v}_i = \emptyset$. In the following, we show how to obtain exact transition matrices for the case of the Hénon map.

A finite representation can be simplified by removing boxes having empty intersection with the invariant part of Ω . We remove boxes \mathbf{v}_i for which $A_{j,i} = 0$ for all $1 \leq j \leq N$ and boxes \mathbf{v}_j for which $A_{j,i} = 0$ for all $1 \leq i \leq N$. This process is continued until no more boxes can be removed. Similarly, one can remove boxes not belonging to the recurrent set of f . This is done by removing boxes which do not belong to any closed path allowed by A . Removing the non-invariant part and the non-recurrent part reduces the number of boxes in the cover and simplifies the transition matrix without changing the topological entropy.

From a finite representation (V, A) of f with the accuracy ε we may produce a finite representation with the accuracy $\varepsilon/2$. This is done by splitting each ε -box in V into 2^m boxes with size $\varepsilon/2$ and repeating the computations described above (see also [Dellnitz *et al.*, 1997], where the subdivision algorithm to obtain outer approximations of invariant sets by box covers is presented).

Finite representations obtained in the process described above may significantly overestimate the attractor. More accurate enclosures for a given box size ε may be obtained from finer representations by the *box merging* method. In this method, one first computes a finite representation (W, B) with boxes of size $\varepsilon/2^k$ for some $k > 1$ and then merges boxes from W to obtain a finite representation (V, A) with the accuracy ε . The transition matrix A is computed directly from the transition matrix B without recalculating the images of ε -boxes. It will be shown in Section 3 that this method permits obtaining very accurate enclosures of attractors.

The finite representation (V, A) represents the dynamics of f with the accuracy ε . If two trajectories $(x_k), (y_k)$ of a given length follow the same sequence of boxes then they cannot be distinguished by this representation. We are interested in computing the number of trajectories of a given length n which can be distinguished by a given finite representation. Such trajectories constitute an (n, ε) -separated set for the map f over Ω .

Let us discuss how to compute the number P_n of paths of length n which are admissible by the transition matrix A . The key observation is that P_n is equal to the sum of elements of A^n , i.e. $P_n = \sum_{i=1}^N \sum_{j=1}^N (A^n)_{i,j}$. Let us denote by $P_{n,j}$ the number of admissible paths of length n starting in \mathbf{v}_j . Since there is a single path of zero length starting in each box we assign $P_{0,j} = 1$ for $1 \leq j \leq N$. $P_{n,j}$ for $n > 0$ and $1 \leq j \leq N$ can be found recursively using the formula

$$P_{n,j} = \sum_{i=1}^N A_{j,i} P_{n-1,i} = \sum_{i \in D_j} P_{n-1,i}, \quad (7)$$

where $D_j = \{i: A_{j,i} = 1\}$. The number P_n of admissible paths of length n is then computed as

$$P_n = \sum_{j=1}^N P_{n,j}. \quad (8)$$

The complexity of the algorithm is of order $(N + C) \cdot n$, where N is the number of boxes and C is the number of non-forbidden connections (or the number of non-zero entries in A). The algorithm is fast and can be used for relatively large n .

The number P_n can be used to compute an estimate of the topological entropy of the finite representation

$$H_F(f, n, \varepsilon) = \frac{1}{n} \log P_n = \frac{1}{n} \log \sum_{i=1}^N \sum_{j=1}^N A^n. \quad (9)$$

Let us assume that A has a dominant eigenvalue, i.e. an eigenvalue which is strictly greater in magnitude than other eigenvalues. Under this assumption, to compute the limit of $H_F(f, n, \varepsilon)$ when n goes to infinity one can use the following formula

$$H_F(f, \infty, \varepsilon) = \lim_{n \rightarrow \infty} \frac{1}{n} \log \sum_{i=1}^N \sum_{j=1}^N A^n = \log |\lambda_1|, \quad (10)$$

where λ_1 is the dominant eigenvalue of A . Formula (10) follows from $\sum_{i=1}^N \sum_{j=1}^N A^n = E^\top A^n E = c_1^2 \lambda_1^n + \dots + c_N 2 \lambda_N^n$, where λ_k are eigenvalues of A with corresponding eigenvectors u_k , and $E^\top = (1, 1, \dots, 1)^\top = c_1 u_1 + \dots + c_N u_N$ (compare [Golub & Loan, 2013]).

The dominant eigenvalue λ_1 can be found using the Rayleigh's power method (see [Golub & Loan, 2013]). The power iteration algorithm starts with a random vector b_0 . At every iteration, the vector b_k is multiplied by A and normalized, i.e. $b_{k+1} = \frac{Ab_k}{\|Ab_k\|}$. The sequence $\mu_k = \frac{b_k^\top Ab_k}{b_k^\top b_k}$ converges to λ_1 and b_k converges to the corresponding eigenvector u_1 under the assumption that A has a dominant eigenvalue λ_1 and that b_0 has a nonzero component in the direction u_1 .

For large n and small ε the estimate $H_F(f, n, \varepsilon)$ is an upper bound on $H(f, n, \varepsilon)$ defined in (4) and $H_F(f, \infty, \varepsilon)$ is an upper bound on $H(f, \varepsilon)$ defined in (5). As it will be shown in the following section, the topological entropy of a finite approximation may be significantly larger than the topological entropy of the map. The reason is that even if a given path is allowed by the transition matrix it does not necessarily imply that there exist a trajectory following this path. For example, for a given path $(\mathbf{v}_{i_1}, \mathbf{v}_{i_2}, \mathbf{v}_{i_3})$ it may happen that $f(\mathbf{v}_{i_1}) \cap f^{-1}(\mathbf{v}_{i_3}) = \emptyset$ although $f(\mathbf{v}_{i_1}) \cap \mathbf{v}_{i_2} \neq \emptyset$ and $f(\mathbf{v}_{i_2}) \cap \mathbf{v}_{i_3} \neq \emptyset$.

A method to reduce this effect is to construct finite approximations of iterates of the map f . In this approach using a finite representation (V, A) of f we compute a finite representation (V, B) of f^k for some $k > 1$. Note that the transition matrix B can be generated directly from A without the evaluation of f^k . We set $B_{j,i} = 1$ if and only if there is an admissible path of length k starting at \mathbf{v}_j and ending at \mathbf{v}_i . The relation between the topological entropy of the map f and the topological entropy of f^k is $H(f^k) = k \cdot H(f)$ (compare [Adler *et al.*, 1965]). Hence, an approximation of the topological entropy of f can be calculated as $k^{-1} H_F(f^k, \infty, \varepsilon) = k^{-1} \log \lambda_1$, where λ_1 is the dominant eigenvalue of B . This method can be combined with the box merging technique, to obtain better upper bounds on the topological entropy.

3. Numerical results

Here, the methods presented in Section 2 are applied to compute the topological entropy of finite representations of the Hénon map. The *Hénon map* [Hénon, 1976] is a two-parameter map of a plane into itself

$$h(x, y) = (1 + y - ax^2, bx), \quad (11)$$

displaying a wide array of dynamical behaviors as its parameters are varied. We consider the classical parameter values $a = 1.4$, $b = 0.3$, for which the famous Hénon attractor is observed in simulations. The problem whether the attractor is chaotic remains an open problem (compare [Galias & Tucker, 2015]).

Using the linear change of coordinates $(x, y) \mapsto (\bar{y}, b\bar{x})$ converts (11) to

$$h(x, y) = (y, 1 - ay^2 + bx). \quad (12)$$

In computations, we will use this version of the Hénon map because it permits a more efficient implementation. An ε -box $\mathbf{v} = (\mathbf{v}_1, \mathbf{v}_2) = [k_1\varepsilon, (k_1 + 1)\varepsilon] \times [k_2\varepsilon, (k_2 + 1)\varepsilon]$ is represented as a pair of numbers (k_1, k_2) . The image of the box (k_1, k_2) under the map (12) is a set of boxes with the first coordinate being $l_1 = k_2$ and the second coordinate $l_2 \in \{l'_2, l'_2 + 1, \dots, l''_2\}$, where $[l'_2\varepsilon, l''_2\varepsilon]$ is the smallest interval enclosing $1 - av_2^2 + bv_1$. It follows that there is no numerical error in the computation of the first coordinate. Apart from a very rare situation that the endpoints of the interval $1 - av_2^2 + bv_1$ are located closer to borders between ε -boxes than the machine accuracy we also make no numerical error when computing the second coordinate of the box (k_1, k_2) . In consequence, the map (12) permits obtaining finite representations free from numerical errors.

The method described in Section 2 is used to construct finite representations of the Hénon attractor. First, the rectangle $[-1.5, 1.5] \times [-1.5, 1.5]$ is covered by 36 ε -boxes of size $\varepsilon = 0.5$. Removing the non-invariant part results in the cover V composed of 22 boxes and the transition matrix A with 60 non-zero entries. Finite representations with the accuracy $\varepsilon = 2^{-p}$ for $p = 2, 3, \dots, 20$ are found recursively for increasing p . The number of boxes in finite representations for different accuracies ε are reported in Table 1 in the column labeled “box splitting”. The finest representation is obtained for the accuracy $\varepsilon = 2^{-20}$. To simplify finite representations for $\varepsilon > 2^{-20}$ the method of box merging is used. We start from the finite representation with the accuracy $\varepsilon = 2^{-20}$ and recursively merge covers and calculate transition matrices to obtain finite representations with the accuracy $2^{-19}, 2^{-18}, \dots, 2^{-1}$. The results are presented in Table 1 in the column labeled “box merging”. The number of boxes is reduced by more than 14% for $p = 2, 3, \dots, 15$. The largest reduction of 28% is observed for $p = 7$. Covers with ε -boxes for $\varepsilon = 2^{-4}$ and $\varepsilon = 2^{-7}$ are shown in Fig. 1 in gray and blue, respectively.

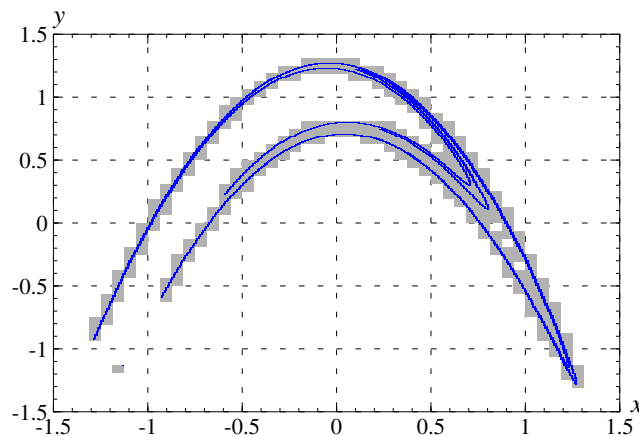


Fig. 1. Covers with ε -boxes for $\varepsilon = 2^{-4}$ (gray) and $\varepsilon = 2^{-7}$ (blue).

To assess the quality of the results, covers of the numerically observed attractor with ε -boxes for $\varepsilon = 2^{-18}$ are found. 1000 trajectories of the length 10^{10} or $2 \cdot 10^{10}$ with initial positions selected randomly from the set $[-0.1, 0.1] \times [-0.1, 0.1]$ are computed. In each case 10^6 iterations are skipped to reach the steady state and the remaining points are used to find the cover of the attractor by ε -boxes. The total number of ε -boxes visited in all 1000 runs is 52 549 484. It is interesting to note that in 230 cases a trajectory reaches a periodic steady state. The reason for observing a periodic steady state is that the calculations are carried out in the double precision arithmetic. Each trajectory point (x, y) is stored as a pair of numbers representable in the double precision arithmetic. In consequence, the state space is discrete

and each trajectory has to be eventually periodic. It is a bit surprising that period are small compared to the size of the state space. The periods found are 140 522 953, 323 659 552, 353 107 615, 1 210 581 335, and 2 875 179 482. From the discussion presented above, it follows that in order to cover the attractor by ε -boxes, we should compute several trajectories. If we compute a single trajectory it may converge to a periodic steady state and after the convergence no more ε -boxes are found. For example, if we start from the initial conditions $(x, y) = (0.63945820192020463857, 0.54992529646318766279)$ which in double-precision arithmetic is periodic with the period 140 522 953, then we detect only 39 169 990 ε -boxes which is significantly less than the total number 52 549 484 of ε -boxes found.

Covers with boxes of larger size are found from the cover with box size $\varepsilon = 2^{-18}$ via the box merging technique. Cover sizes obtained using this procedure are reported in Table 1 in the column labeled “attractor cover”. These results may be treated as a lower bound on the number for ε -boxes covering the attractor. It may happen, especially for small ε that in spite of using a very large number of iterations not all ε -boxes covering the attractor are visited by generated trajectories. For $\varepsilon = 2^{-10}$ all 45561 ε -boxes are detected in each of 1000 runs. For $\varepsilon = 2^{-11}$ each ε -box is detected in at least 155 runs. For $\varepsilon \leq 2^{-12}$ at least one of the ε -boxes is detected in a single run only. This indicates that the covers obtained using the attractor cover method are true covers for $\varepsilon \geq 2^{-11}$. On the other hand it is very likely that covers obtained for $\varepsilon \leq 2^{-12}$ are incomplete. Note that for $p \leq 8$ there is a difference of one ε -box in covers obtained using the box merging and the attractor cover methods. The attractor cover does not contain the box enclosing the unstable fixed point $(x, y) \approx (-1.13135, -1.13135)$, which belongs to the invariant part of the rectangle $[-1.5, 1.5] \times [-1.5, 1.5]$. Since the box merging method produces an enclosure of the attractor cover it follows that covers obtained for $p \leq 8$ are exact. For $p \leq 14$, the results obtained using the box merging method are very close to the results found by covering the attractor. The difference in the number of boxes is below 0.3%. This shows that the box merging approach is successful in obtaining accurate attractor covers.

Table 1. The number N of ε -boxes in covers obtained using different methods and the corresponding approximation of the box-counting dimension \dim_{box} .

ε	box splitting		box merging		attractor cover	
	N	\dim_{box}	N	\dim_{box}	N	\dim_{box}
2^{-1}	22	4.4594	20	4.3219	19	4.2479
2^{-2}	57	2.9164	48	2.7925	47	2.7773
2^{-3}	135	2.3589	111	2.2648	110	2.2605
2^{-4}	320	2.0805	258	2.0028	257	2.0014
2^{-5}	805	1.9306	607	1.8491	606	1.8486
2^{-6}	1952	1.8218	1437	1.7481	1436	1.7480
2^{-7}	4595	1.7380	3324	1.6712	3323	1.6712
2^{-8}	9928	1.6597	7792	1.6160	7791	1.6159
2^{-9}	23001	1.6099	19064	1.5798	19061	1.5798
2^{-10}	54295	1.5729	45573	1.5476	45561	1.5476
2^{-11}	129098	1.5435	111036	1.5237	110992	1.5236
2^{-12}	317626	1.5231	271874	1.5044	271666	1.5043
2^{-13}	751942	1.5016	649739	1.4853	648840	1.4852
2^{-14}	1828895	1.4859	1578034	1.4707	1573698	1.4704
2^{-15}	4412827	1.4716	3782436	1.4567	3760354	1.4562
2^{-16}	10526788	1.4580	9138053	1.4452	9038525	1.4442
2^{-17}	25736445	1.4481	22537436	1.4368	22052165	1.4350
2^{-18}	61227270	1.4371	54780599	1.4282	52549484	1.4248
2^{-19}	149836455	1.4294	140166639	1.4243		
2^{-20}	367252401	1.4226	367252401	1.4226		

Having an accurate cover of the Hénon attractor we may compute approximations of its box-counting

dimension. The *box-counting dimension* of the set S is defined as

$$\dim_{\text{box}}(S) = \lim_{\varepsilon \rightarrow 0} \frac{N(\varepsilon)}{\log(1/\varepsilon)}, \quad (13)$$

where $N(\varepsilon)$ is the number of boxes of side length ε required to cover the set S .

Approximations obtained for covers with ε -boxes of size $\varepsilon = 2^{-p}$ for $p = 1, 2, \dots, 20$ computed for covers obtained using three different methods are reported in Table 1 and shown in Fig. 2. One can see that approximations obtained using the box merging method are close to the ones found by covering the attractor by ε -boxes. The box splitting method gives an overestimation clearly visible especially in the range $p \leq 10$.

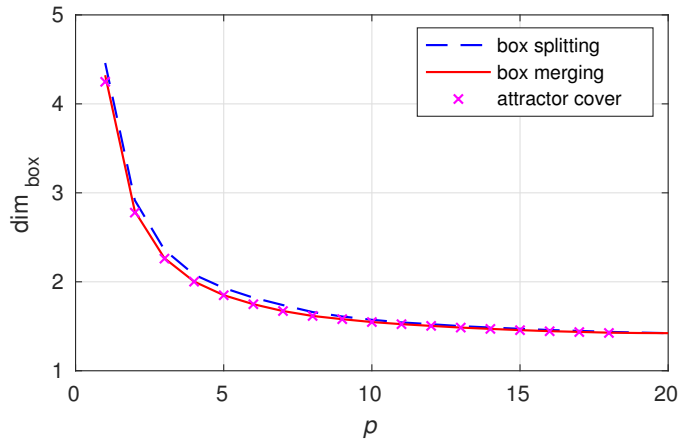


Fig. 2. Approximations of the box-counting dimension for covers of the Hénon attractor by ε -boxes with $\varepsilon = 2^{-p}$.

Now, we present results on the topological entropy of finite representations of the Hénon map. First, let us consider finite representations with the accuracy $\varepsilon = 2^{-7}$. The number P_n of paths of lengths $n \leq 10000$ is computed using formulas (7) and (8). Estimates $H_F(h, n, \varepsilon)$ based on the number of paths are computed using formula (9). The computation time is 7.71 seconds using a single core 3.4 GHz processor. The limit $H_F(h, \infty, \varepsilon)$ is computed using (10). 150 iteration of the Rayleigh's power method are sufficient to find the dominant eigenvalue. The computation time is 0.1 seconds. The results are presented in Table 2. One can see that the convergence of $H_F(h, n, \varepsilon)$ when n goes to infinity is relatively slow. For $n = 100$ and $n = 1000$ the relative difference between $H(f, n, \varepsilon)$ and the limit $H(f, \infty, \varepsilon)$ is 7% and 0.8%, respectively. These results show that estimating the topological entropy using formula (10) combined with the power method to find the dominant eigenvalue is faster than the method based on computing the number of paths.

In a similar way, the limits $H_F(h, \infty, \varepsilon)$ are computed for finite representations with different box sizes. The results are presented in Table 3. For each box size $\varepsilon = 2^{-p}$, $p \in \{1, 2, \dots, 20\}$ we report the number N of ε -boxes in the cover, the number C of non-zero entries in the transition matrix and the topological entropy $H_F(h, \infty, \varepsilon)$ of the finite representation found using formula (10).

In the first part of Table 3, we present the results obtained using the box splitting method. One can see that the convergence of $H_F(h, \infty, \varepsilon)$ when ε is decreased is relatively fast. For $p \geq 10$ the results belong to the interval $[1.1105, 1.1112]$. This indicates that the topological entropy stabilizes when the box size is decreased. It follows that it is sufficient to study the topological entropy of a finite representation with a relatively low accuracy to get a good description of complexity of trajectories. In the second part of Table 3 we present results obtained using the box merging method. The first observation is that the topological entropy is significantly smaller than in the first case. This confirms that the box merging procedure permits obtaining a more accurate description of the dynamics of the map which results in a significant reduction of the topological entropy of a finite representation. In this case, $H_F(h, \infty, \varepsilon)$ belongs to the interval $[0.8509, 0.8717]$ for $9 \leq p \leq 15$. The increase for $p \geq 16$ is caused by the fact that the box

Table 2. The number of paths P_n and estimates $H_F(h, n, \varepsilon) = n^{-1} \log P_n$ of the topological entropy for finite representations of h with the accuracy $\varepsilon = 2^{-7}$.

n	box splitting		box merging	
	P_n	$H_F(h, n, \varepsilon)$	P_n	$H_F(h, n, \varepsilon)$
0	4595	∞	3324	∞
1	14100	9.5539	7181	8.8792
2	42489	5.3285	16559	4.8573
3	128899	3.9223	38166	3.5166
4	391829	3.2196	88550	2.8478
5	1197093	2.7991	205877	2.4470
7	10956372	2.3156	1081119	1.9848
10	309723491	1.9551	12950681	1.6377
20	$2.1025 \cdot 10^{13}$	1.5338	$5.2644 \cdot 10^{10}$	1.2343
50	$6.5690 \cdot 10^{27}$	1.2810	$3.5088 \cdot 10^{21}$	0.9922
100	$9.4506 \cdot 10^{51}$	1.1968	$3.8433 \cdot 10^{39}$	0.9115
200	$1.9560 \cdot 10^{100}$	1.1546	$4.6109 \cdot 10^{75}$	0.8711
500	$1.7343 \cdot 10^{245}$	1.1294	$7.9624 \cdot 10^{183}$	0.8469
1000	$6.5878 \cdot 10^{486}$	1.1209	$1.9791 \cdot 10^{364}$	0.8388
2000	$9.5049 \cdot 10^{969}$	1.1167	$1.2228 \cdot 10^{725}$	0.8348
5000	$2.8547 \cdot 10^{2419}$	1.1142	$2.8836 \cdot 10^{1807}$	0.8324
10000	$1.7847 \cdot 10^{4835}$	1.1134	$2.5957 \cdot 10^{3611}$	0.8316
∞	∞	1.1125	∞	0.8308

 Table 3. The topological entropy $H_F(h, \infty, \varepsilon)$ of finite representations with the accuracy $\varepsilon = 2^{-P}$.

ε	box splitting			box merging		
	N	C	H_F	N	C	H_F
2^{-1}	22	60	1.0125	20	41	0.8319
2^{-2}	57	164	1.0780	48	95	0.7880
2^{-3}	135	391	1.0896	111	222	0.8256
2^{-4}	320	940	1.0890	258	539	0.8348
2^{-5}	805	2397	1.1111	607	1270	0.8378
2^{-6}	1952	5927	1.1137	1437	3097	0.8371
2^{-7}	4595	14100	1.1125	3324	7181	0.8308
2^{-8}	9928	30498	1.1110	7792	17141	0.8464
2^{-9}	23001	70245	1.1124	19064	41879	0.8614
2^{-10}	54295	164301	1.1111	45573	100746	0.8717
2^{-11}	129098	392380	1.1109	111036	247160	0.8673
2^{-12}	317626	974431	1.1112	271874	595847	0.8589
2^{-13}	751942	2323976	1.1111	649739	1434256	0.8509
2^{-14}	1828895	5686097	1.1110	1578034	3507123	0.8566
2^{-15}	4412827	13643148	1.1110	3782436	8533209	0.8702
2^{-16}	10526788	32763055	1.1106	9138053	21254741	0.8860
2^{-17}	25736445	80423896	1.1105	22537436	53624056	0.9138
2^{-18}	61227270	190788081	1.1105	54780599	138896360	0.9684
2^{-19}	149836455	464208748	1.1105	140166639	385320220	1.0364
2^{-20}	367252401	1126053561	1.1105	367252401	1126053561	1.1105

merging procedure requires a certain number of merging levels to improve the results.

Now, we present results obtained for finite representations of iterates of the Hénon map. First, using a finite representation (V, A) of h with the accuracy ε , we generate the finite representation (V, B) of h^k ($k \geq 2$) with the same accuracy ε . In the transition matrix B for the k th iteration we set $B_{j,i} = 1$ if and only if v_i can be reached from v_j in exactly k steps. The logarithm of the dominant eigenvalue of B is the topological entropy of the finite representation of h^k . An estimate of the topological entropy of the map h is obtained by dividing the result by k . Using the box merging technique, we recursively generate finite

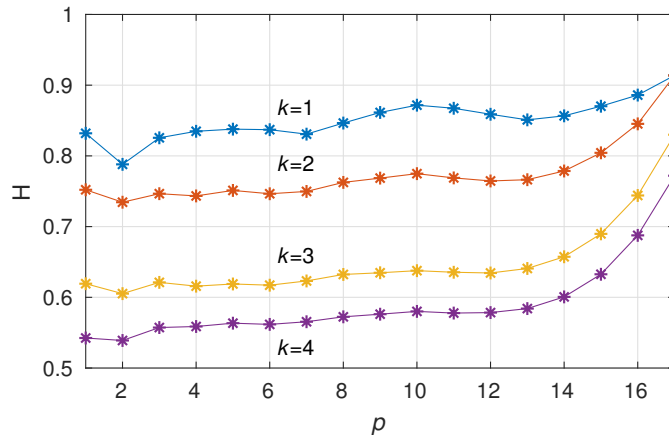
Table 4. The topological entropy of finite representations of h^4 versus the accuracy ε .

ε	N	C	$H_F(h^k, \infty, \varepsilon)$	$k^{-1} H_F(h^k, \infty, \varepsilon)$
2^{-1}	20	140	2.1698	0.5425
2^{-2}	48	351	2.1558	0.5390
2^{-3}	111	850	2.2291	0.5573
2^{-4}	258	2043	2.2349	0.5587
2^{-5}	607	4905	2.2537	0.5634
2^{-6}	1437	12060	2.2468	0.5617
2^{-7}	3324	28444	2.2618	0.5655
2^{-8}	7792	69569	2.2896	0.5724
2^{-9}	19064	171435	2.3046	0.5761
2^{-10}	45573	416900	2.3204	0.5801
2^{-11}	111036	1035760	2.3109	0.5777
2^{-12}	271874	2514956	2.3136	0.5784
2^{-13}	649739	6272146	2.3363	0.5841
2^{-14}	1578034	16506852	2.4024	0.6006
2^{-15}	3782436	45473785	2.5303	0.6326
2^{-16}	9138053	140964052	2.7504	0.6876
2^{-17}	22537436	498247791	3.0878	0.7720

representations of h^k with the accuracy $2^j\varepsilon$ for $j = 1, 2, 3, \dots$ and compute estimates of the topological entropy.

The topological entropy of finite representations of the fourth iterate of the Hénon map based on the finite representation of h with the accuracy $\varepsilon = 2^{-17}$ are reported in Table 4. One can see that the results are smaller than the ones given in Table 3. This shows that carrying out calculations for the k th iterate of a map with $k > 1$ may produce a better upper bound on the topological entropy of the map.

Similar computations are carried out for the second and the third iterate of the Hénon map. The results are plotted in Fig. 3. For each finite representation of h^k with the box size $\varepsilon = 2^{-p}$, $p = 1, 2, \dots, 17$, we plot the rescaled topological entropy (i.e., the topological entropy divided by k). For comparison, we also plot the topological entropy of finite representations of h ($k = 1$). One can see that the rescaled topological entropy decreases with k . It is interesting to note that the results obtained for $p \leq 12$ do not vary much. Practically, the complexity of finite representations is independent on the accuracy of the finite representation. An increase for $p > 12$ is caused by the fact that the box merging techniques requires several iterations to work properly.

Fig. 3. Rescaled topological entropy of finite representations of h^k for $k = 1, 2, \dots, 4$ with the accuracy $\varepsilon = 2^{-p}$.

Computing finite representations of h^k for $k > 4$ based on the finite representation of h with the accu-

racy $\varepsilon = 2^{-17}$ becomes difficult because of increasing memory requirements. When h grows the transition matrix for the k th iterate becomes less sparse and more memory is necessary to store the finite representation. Therefore, computations for $k > 4$ are carried out based on the cover with ε -boxes of size $\varepsilon = 2^{-14}$. Results obtained for $k = 1, 2, \dots, 10$ are plotted in Fig. 4. One can see that the results are larger than the ones presented in Fig. 3, especially for $p > 10$. This shows that if we want to obtain reliable results we need to start with sufficiently small boxes and use the box merging technique to reduce finite representations. It is interesting to note that for $k > 4$ the plots drop for small p . This is caused by incapability of obtaining good representations with large boxes when the iterate k is high. For fixed ε increasing k increases the number of nonzero entries in the transition matrix. Eventually, all or almost all entries become nonzero (for chaotic maps the number of boxes which can be reached from a given box after k iterations grows exponentially with k). The number of nonzero entries which are added when k is increased cannot compensate for the drop caused by dividing by k . To estimate what is the maximum size of ε -boxes for a given k let us note that the dominant eigenvalue of a transition matrix $A \in \mathbb{R}^{N \times N}$ cannot be larger than N . It follows that the number of boxes has to be larger than $N = \exp(kH)$, where H is an expected value of the topological entropy of the map. Knowing N we can estimate the maximum box size from Table 1. For example, for $k = 10$ assuming $H = 0.5$ we obtain $N > 150$ and $\varepsilon \leq 2^{-4}$. In practice, one has to use much smaller ε -boxes to obtain reliable results.

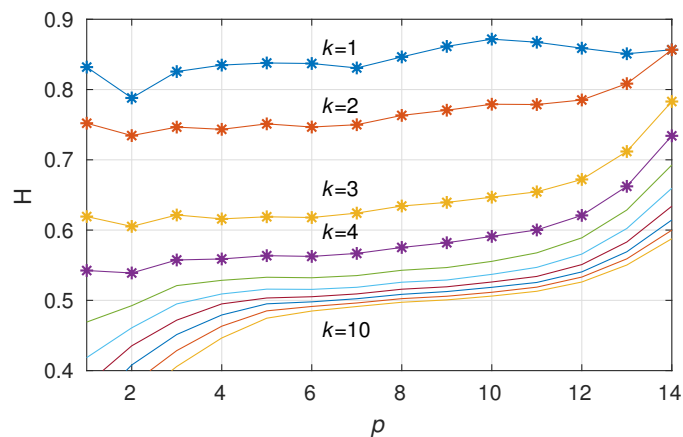


Fig. 4. Rescaled topological entropy of finite representations of h^k for $k = 1, 2, \dots, 10$ with the accuracy $\varepsilon = 2^{-p}$.

4. Conclusions

Efficient methods for the computation of the topological entropy of finite representations of nonlinear maps have been proposed. Accurate finite approximations of the Hénon map h and its iterates h^k for $2 \leq k \leq 10$ have been constructed. It has been shown that the box merging technique permits obtaining very accurate finite representations. The topological entropy of finite representation of the Hénon map has been computed. It has been shown that the topological entropy of a finite representation is significantly larger than the topological entropy $H(h)$ of h and that the difference is practically independent on the accuracy ε of the finite representations for ε sufficiently small.

It has been also shown that considering iterates h^k produces upper bounds on the topological entropy of h which decrease with k . We believe that these bounds for sufficiently large k together with the results presented in [Yomdin, 1991] may be used to obtain nontrivial upper bounds on $H(h)$. This will be the subject of future studies.

Acknowledgments

This work is supported by the AGH University of Science and Technology. The author would like to thank Prof. Marian Mrozek and Dr. Mateusz Juda for providing access to a computer box with 250 GB of memory,

which was used to compute the finite approximation of the Hénon map with the accuracy $\varepsilon = 2^{-20}$.

References

- Adler, R. L., Konheim, A. G. & McAndrew, M. H. [1965] “Topological entropy,” *Trans. Amer. Math. Soc.* **114**, 309–319.
- Akgul, A., Kacar, S., Aricioglu, B. & Pehlivan, I. [2013] “Text encryption by using one-dimensional chaos generators and nonlinear equations,” *2013 8th International Conference on Electrical and Electronics Engineering (ELECO)*, pp. 320–323.
- Arai, Z. [2007] “On hyperbolic plateaus of the Hénon map,” *Experimental Mathematics* **16**, 181–188.
- Auerbach, D., Cvitanović, P., Eckmann, J., Gunaratne, G. & Procaccia, I. [1987] “Exploring chaotic motion through periodic orbits,” *Phys. Rev. Lett.* **58**, 2387–2389.
- Biham, O. & Wenzel, W. [1989] “Characterization of unstable periodic orbits in chaotic attractors and repellers,” *Physical Review Letters* **63**, 819–822.
- Bollt, E. M., Stanford, T., Lai, Y. C. & Życzkowski, K. [2001] “What symbolic dynamics do we get with a misplaced partition? On the validity of threshold crossings analysis of chaotic time-series,” *Physica D* **154**, 259–286.
- Bowen, R. [1971] “Entropy for group endomorphisms and homogeneous spaces,” *Trans. Amer. Math. Soc.* **153**, 401–414.
- Cicek, I., Pusane, A. E. & Dundar, G. [2017] “An integrated dual entropy core true random number generator,” *IEEE Transactions on Circuits and Systems II: Express Briefs* **64**, 329–333.
- D’Alessandro, G., Grassberger, P., Isola, S. & Politi, A. [1999] “On the topology of the Hénon map,” *Journal of Physics A: Mathematical and General* **23**, 5285.
- Day, S., Frongillo, R. & Trevino, R. [2008] “Algorithms for rigorous entropy bounds and symbolic dynamics,” *SIAM J. Applied Dynamical Systems* **7**, 1477–1506.
- Dellnitz, M., Hohmann, A., Junge, O. & Rumpf, M. [1997] “Exploring invariant sets and invariant measures,” *Chaos: Interdiscipl. J. Nonlinear Sci.* **7**, 221–228.
- Dinaburg, E. I. [1971] “On the relations among various entropy characteristics of dynamical systems,” *Izv. Akad. Nauk SSSR Ser. Mat.* **35**, 324–366.
- Frongillo, R. [2014] “Topological entropy bounds for hyperbolic plateaus of the Hénon map,” SIAM Undergraduate Research Online, <http://www.siam.org/students/siuro/vol7/S01271.pdf>.
- Froyland, G., Junge, O. & Ochs, G. [2001] “Rigorous computation of topological entropy with respect to a finite partition,” *Physica D* **154**, 68–84.
- Galias, Z. [2001] “Interval methods for rigorous investigations of periodic orbits,” *Int. J. Bifurcation and Chaos* **11**, 2427–2450.
- Galias, Z. [2002] “Obtaining rigorous bounds for topological entropy for discrete time dynamical systems,” *Proc. Int. Symp. Nonl. Theory Appl. (NOLTA) (Xi’an, PRC)*, pp. 619–622.
- Galias, Z. & Tucker, W. [2015] “Is the Hénon attractor chaotic?” *Chaos: An Interdisciplinary Journal of Nonlinear Science* **25**, 033102 (12 pages).
- Galias, Z. & Zgliczyński, P. [2001] “Abundance of homoclinic and heteroclinic orbits and rigorous bounds for the topological entropy for the Hénon map,” *Nonlinearity* **14**, 909–932.
- Golub, G. & Loan, C. V. [2013] *Matrix computations* (Johns Hopkins University Press, Baltimore).
- Grassberger, P. & Kantz, H. [1985] “Generating partitions for the dissipative Hénon map,” *Physica* **17D**, 235–238.
- Grassberger, P., Kantz, H. & Moenig, U. [1989] “On the symbolic dynamics of the Hénon map,” *J. Physics A* **22**, 5217–5230.
- Guo, X. X., Xiang, S. Y., Zhang, Y. H., Wen, A. J. & Hao, Y. [2018] “Information-theory-based complexity quantifier for chaotic semiconductor laser with double time delays,” *IEEE Journal of Quantum Electronics* **54**, 1–8.
- Hénon, M. [1976] “A two dimensional map with a strange attractor,” *Communications in Mathematical Physics* **50**, 69–77.
- Hirata, Y. & Mees, A. I. [2003] “Estimating topological entropy via a symbolic data compression technique,”

- Physical Review E* **67**, 026205.
- Jacobs, J., Ott, E. & Hunt, B. R. [1998] “Calculating topological entropy for transient chaos with an application to communicating with chaos,” *Physical Review E* **57**, 6577.
- Misiurewicz, M. & Szewc, B. [1980] “Existence of a homoclinic point for the Hénon map,” *Comm. Math. Phys.* **75**, 285–291.
- Newhouse, S., Berz, M., Grote, J. & Makino, K. [2008] “On the estimation of topological entropy on surfaces,” *Contemp. Math.* **469**, 243–270.
- Newhouse, S. & Pignataro, T. [1993] “On the estimation of topological entropy,” *Journal of Statistical Physics* **72**, 1331–1351.
- Newhouse, S. E. [1988] “Entropy and volume,” *Ergod. Th. Dynam. Sys.* **8**, 283–299.
- Qi, T., Jun-min, J. & Jun-li, J. [2016] “An image encryption algorithm based on high-dimensional chaotic systems,” *IEEE Int. Conference on Signal Processing, Communications and Computing (ICSPCC)*, pp. 1–4.
- Robinson, C. [1995] *Dynamical Systems: Stability, Symbolic Dynamics, and Chaos* (CRC Press, Boca Raton, FL, USA).
- Stoffer, D. & Palmer, K. [1999] “Rigorous verification of chaotic behavior of maps using validated shadowing,” *Nonlinearity* **12**, 1683–1698.
- Yomdin, Y. [1991] “Local complexity growth for iterations of real analytic mappings and semicontinuity moduli of the entropy,” *Ergodic Theory and Dynamical Systems* **11**, 583–602.
- Zgliczyński, P. [1997] “Computer assisted proof of chaos in the Rössler equations and the Hénon map,” *Nonlinearity* **10**, 243–252.
- Zhou, T., Zhou, Z., Yu, M. & Ye, Y. [2006] “Design of a low power high entropy chaos-based truly random number generator,” *IEEE Asia Pacific Conference on Circuits and Systems*, pp. 1955–1958.